frontiers in Nanotechnology

REVIEW
published: 25 August 2021
doi: 10.3389/fnano.2021.732916

Two-Dimensional Van Der Waals Materials for Spin-Orbit Torque Applications

Mingming Tian[1], Yonghui Zhu[1,2], Milad Jalali[1], Wei Jiang[1], Jian Liang[1], Zhaocong Huang[1], Qian Chen[2], Zhongming Zeng[2] and Ya Zhai[1]**

[1]School of Physics, Southeast University, Nanjing, China, [2]Key Laboratory of Multifunctional Nanomaterials and Smart Systems, Suzhou Institute of Nano-Tech and Nano-Bionics, Chinese Academy of Sciences, Suzhou, China

Spin-orbit torque (SOT) provides an efficient approach to control the magnetic state and dynamics in different classes of materials. Recent years, the crossover between two-dimensional van der Waals (2D vdW) materials and SOT opens a new prospect to push SOT devices to the 2D limit. In this mini-review, we summarize the latest progress in 2D vdW materials for SOT applications, highlighting the comparison of the performance between devices with various structures. It is prospected that the large family of 2D vdW materials and numerous combinations of heterostructures will widely extend the material choices and bring new opportunities to SOT devices in the future.

Keywords: spin-orbit torque, two-dimensional, van der waals materials, magnetic heterostructure, spin Hall effect, rashba effect

OPEN ACCESS

Edited by:
P.K. Johnny Wong, Northwestern Polytechnical University, China

Reviewed by:
Giovanni Vinai, Consiglio Nazionale delle Ricerche (CNR), Italy
Chi Wah Leung, Hong Kong Polytechnic University, Hong Kong, SAR China

****Correspondence:***
Ya Zhai
yazhai@seu.edu.cn
Qian Chen
qchen2016@sinano.ac.cn

Specialty section:
This article was submitted to Nanodevices, a section of the journal Frontiers in Nanotechnology

Received: *29 June 2021*
Accepted: *10 August 2021*
Published: *25 August 2021*

Citation:
Tian M, Zhu Y, Jalali M, Jiang W, Liang J, Huang Z, Chen Q, Zeng Z and Zhai Y (2021) Two-Dimensional Van Der Waals Materials for Spin-Orbit Torque Applications. Front. Nanotechnol. 3:732916. doi: 10.3389/fnano.2021.732916

BACKGROUND

The recently developed spin-orbit torque (SOT) provides an ultrafast and energy-efficient method to manipulate magnetization by electric-current (Soumyanarayanan et al., 2016; Qiu et al., 2018; Cao et al., 2020b; Hidding and Guimarães, 2020; Han et al., 2021). Owing to potential advantages including low power consumption, high density and nonvolatility, SOT devices have attracted widespread attention in various areas such as magnetic random access memory (MRAM) (He et al., 2018), spin Hall nano-oscillator (SHNO) (Zahedinejad et al., 2020) and magnetic nonvolatile logic device (Kurenkov et al., 2019). Conventional SOT devices consist of heavy metal/ferromagnet (HM/FM) bilayers, in which the charge current converts into spin current due to spin-orbit coupling (SOC) effects, and then exerts torques on adjacent ferromagnetic layers. To date, more and more SOT devices based on different classes of materials are reported. Selections of SOT materials has been broadened to magnetic materials (Yang et al., 2020) (Zhou et al., 2020), topological insulators (TIs) (Mellnik et al., 2014), two-dimensional van der Waals (2D vdW) materials (Hidding and Guimarães, 2020) and so on. For further developments, materials with high charge to spin conversion efficiency and high electrical conductivity are pursued.

The crossover between 2D vdW materials and SOTs opens the possibility of pushing spintronic devices to the 2D limit. Some 2D vdW materials, such as transition-metal dichalcogenides (TMDs) are endowed with large SOC and low crystal symmetry, which facilitate to the improvement of SOT efficiency and field-free magnetization switching (Hidding and Guimarães, 2020). Besides, 2D vdW magnets are known to exhibit long-range magnetism (Gong and Zhang, 2019) (Zhang et al., 2019), which are retained even when the thickness of the material is down to the single atomic layer, challenging the Mermin-Wagner theorem (Mermin and Wagner, 1966). Therefore, large SOT efficiency and excellent magnetism are likely to coexist in an atomic-scale SOT device based on 2D

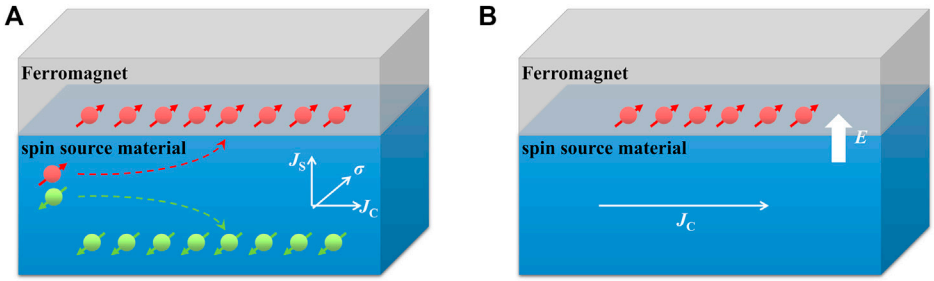

FIGURE 1 | (A) Illustration of the spin Hall effect in the spin source material. **(B)** Illustration of Rashba-Edelstein effect at the interface.

vdW materials. Recent years, emerging studies were carried out on 2D SOT devices. Liu et al. have summarized the recent progress of SOT studies based on transition-metal dichalcogenides (TMDs) and show how these results are in line with the symmetry arguments (Liu and Shao, 2020). Husain et al. reviewed the current progress in research on 2D TMDs for generating SOTs in spin-logic devices (Husain et al., 2020b). Both of them focused on SOT devices based on 2D TMDs. However, the large family of 2D vdW materials and numerous combinations of heterostructures has widely extended the material choices of SOT devices, and there is a lack of overviews of studies on 2D vdW materials beside 2D TMDs for SOT applications.

This review gives an overview of the recent progress on 2D vdW materials for SOT applications. The remainder of this review is structured as follows. We start by introducing the basic principles underlying the physical behaviour of SOT. Then, we outline several magnetic heterostructures based on 2D vdW materials focusing on their pivotal use in SOT devices, including 2D vdW material/FM heterostructures, 2D vdW magnet/HM heterostructures, and all-vdW heterostructures. Additionally, performance modulation of conventional SOT devices by 2D vdW materials is also reviewed. At last, we provide a conclusion and discuss the future perspectives briefly in this field.

ORIGIN OF SOT

SOT phenomenon describes the effect of spin-polarized electrons acting on magnetic moments. The mechanism of SOT can be illustrated from two aspects. Firstly, spin-polarized electrons are generated by an electric current due to SOC effects (Manchon and Zhang, 2009). The main SOC effects attributed to generating spin accumulation are spin Hall effect (SHE) and interface Rashba-Edelstein effect, which will be introduced later. Secondly, the spin polarized electrons exert torques on adjacent magnetic layers, leading to the dissipation, precession or switching of the magnetic moments. Here, we introduce the basic principles underlying the physical behavior of SOTs, including the origin of spin-polarized electrons and the effect of various torques.

The Origin of Spin-Polarized Electrons

Spin Hall Effect

Spin Hall effect (SHE) is one of the most general ways to generate pure spin current in source materials with large SOC using electrical methods. The SHE was theoretically predicted by Dyakonov and Perel (1971) and then be revisited by Hirsch Hirsch (1999) and Zhang Zhang (2000). Although theoretically predicted a long time ago, evidence of SHE had not been experimentally confirmed until 21st century. In 2004, using magneto-optical Kerr microscope, Kato et al. (2004) observed the spin accumulation at the material boundary induced by the SHE in semiconductor GaAs for the first time.

Figure 1A illustrates the mechanism of SHE in a conventional magnetic heterostructure. When an unpolarized charge current J_C is injected into a source material with SOC, electrons with the spin up and down deflect in the opposite direction due to the spin-dependent asymmetric scattering, leading to a transverse spin current J_S perpendicular to the direction of both charge current and the polarization σ of the accumulated spins. Accordingly, the SHE can be represented by

$$\boldsymbol{J}_S = \frac{\hbar}{2e}\theta_{SH}(\boldsymbol{J}_C \times \boldsymbol{\sigma})$$

Where $\hbar$ is the reduced Planck constant divided by 2π, e is the elementary charge, and θ_{SH} is the Spin Hall angle (SHA) (Niimi and Otani, 2015). The value of θ_{SH} determines the charge-spin conversion efficiency of the source material, and the sign of θ_{SH} denotes the polarized direction of spin accumulation at the heterostructure interface. The spin-dependent asymmetric scattering originates from the skew scattering (Niimi et al., 2011), side-jump (Levy et al., 2013), and the intrinsic mechanisms (Zhang, 2000), which are caused by coherent band-mixing effects induced by the external electric field and the disorder potential in the presence of SOC. Therefore, to improve the efficiency of charge-spin conversion, materials with large SOC can be selected as the source of the spin-polarized electrons.

Rashba Effect

Another effective method to generate spin-polarized electrons is the interface current-induced spin accumulation known as the Rashba-Edelstein effect (Dresselhaus, 1955). It was initially

proposed in the context of wurtzite semiconductors and 2D electron gases with broken inversion symmetry (Meijer et al., 2005). Over the last decade, the Rashba-Edelstein effect has been extended to HM/FM structures with broken inversion symmetry (Grytsyuk et al., 2016). Its application for conversion between charge and spin currents has been theoretically predicted and experimentally demonstrated in recent years, as have been reviewed by Koo et al. Koo et al. (2020).

As is illustrated in **Figure 1B**, in structures with broken inversion symmetry, an internal electric field E is generated at the interface along the direction of symmetry breaking due to the potential drop (Manchon, 2020). When the conduction electrons with momentum p move near the interface, an effective magnetic field is induced parallel to $E \times p$. Therefore, the interfacial Rashba effect can be expressed by the following Hamiltonian (Manchon, 2020),

$$H_R = \frac{\alpha_R}{\hbar}(E \times p) \cdot \sigma$$

Where α_R is the Rashba parameter governed by the potential drop at the interface. The Rashba effect results in spin split 2D dispersion surfaces and the spin-momentum locking, which have been investigated across various surfaces and interfaces (Edelstein, 1990). Interface alloying of heavy elements with intermediate-weight metals can enhance the in-plane potential gradient via hybridization, leading to more pronounced Rashba effects, as on the Bi/Ag (111) alloyed interface (Sánchez et al., 2013).

Varieties of Torques

The SOTs induced by spin-polarized electrons act on the precessional magnetization, and the dynamics of the magnetization subject to SOT is governed by the Landau-Lifshitz-Gilbert (LLG) equation,

$$\frac{dM}{dt} = -\gamma M \times H_{eff} + \frac{\alpha}{M_s}\left(M \times \frac{dM}{dt}\right) + \frac{\gamma}{\mu_o M_s}\tau_{SOT}$$

Where τ_{SOT} is the sum of several spin orbit torques (Brataas et al., 2012). Traditionally in materials with mirror symmetries, two kinds of SOTs are proposed, including an out-of-plane field-like torque, $\vec{\xi_{FL}} \propto \hat{m} \times \hat{y}$, and an in-plane damping-like (or Slonczewski) torque, $\vec{\xi_{DL}} \propto \hat{m} \times (\hat{m} \times \hat{y})$ (Miron et al., 2011; Liu et al., 2012a; Avci et al., 2014). In both cases, we define the applied current as always being in the $\hat{y}$ direction, and $\hat{m}$ present the direction of the magnetization. Breaking of the mirror symmetry generates an additional out-of-plane damping-like torque, $\vec{\xi}_{DL,Out-of-plane} \propto \hat{m} \times (\hat{m} \times \hat{y})$ (MacNeill et al., 2017a; MacNeill et al., 2017b; Stiehl et al., 2019a). Recent experiments have demonstrated that $\vec{\xi}_{DL,\ Out-of-plane}$ can be generated using 2D vdW materials like WTe_2 (MacNeill et al., 2017a; MacNeill et al., 2017b) and $MoTe_2$ (Stiehl et al., 2019a) with low crystal symmetry as the spin source material (Stiehl et al., 2019a). This novel SOT holds an excellent promise for field-free switching of the perpendicularly magnetized system.

Apart from these torques, an in-plane field-like torque, $\vec{\xi_T} \propto \hat{m} \times \hat{z}$ is observed in some 2D vdW spin source materials such as $NbSe_2$ (Guimarães et al., 2018). Possible mechanisms contributing to this kind of torque may be the strain-induced symmetry breaking during the fabrication procedure, but further studies are still needed. Recently, another current-induced torque $\xi_C \propto \hat{m} \times \hat{x}$ with Dresselhaus symmetry was observed in $TaTe_2$ (Stiehl et al., 2019b). However, the dominant mechanism behind ξ_C is not the SOT effect but rather the Oersted field due to the resistance anisotropy in 2D materials. Since the Dresselhaus component exists in a wide variety of heterostructures incorporating spin source materials with low crystal symmetries, special attention should be paid to the measurement of SOTs.

It is noted that in systems dominated by the damping-like torque, the value of ξ_{DL} can be equivalent to the SHA. The ratio between SHA and the resistivity of the source material is known as spin Hall conductivity, which is proportional to the power consumption of a SOT device.

CONSTRUCTIONS OF 2D SOT DEVICES

SOT devices based on 2D vdW Materials has been rapidly developed in the last few years. By assorting with material construction, there are mainly three kinds of 2D vdW SOT devices which are based on 2D vdW material/FM heterostructures, 2D vdW magnet/HM heterostructures, and all vdW heterostructures. In this section, we first introduce the preparation methods of 2D vdW materials for SOT devices and then give an overview of 2D vdW SOT devices with different constructions.

Preparing Methods of 2D vdW Materials for SOT Devices

Substantial efforts have been devoted to preparing atomically thin 2D materials with controllable dimensions and thicknesses. Preparing methods of 2D vdW materials for SOT applications mainly includes mechanical exfoliations, chemical vapour deposition (CVD) and magnetron sputtering.

At present, mechanical exfoliations remain the workhorse to prepare 2D vdW materials for SOT studies. Materials prepared by exfoliation techniques are characterized by excellent crystal structures and provide conveniences for controlling the stacking order of 2D materials. In recent years, although various approaches have been reported to enhance the lateral size of exfoliated flakes (Desai et al., 2016; Velický et al., 2018; Huang Y. et al., 2020), the critical limitations of uniform coverage and controlled flake shape restrict its practical applications. On the other hand, by mechanical exfoliation, multiple combinations of van der Waals heterostructures can be stacked, which is beneficial to develop novel SOT devices. However, potential problems such as organic residues, hydrolysis, and oxidation at the interface during exfoliation may become key factors restricting the performance of SOT devices (Zhang et al., 2021).

CVD prevails as the most industry-relevant technique so far. To data, TMDs such as WS_2, WSe_2 and MoS_2 have been prepared by CVD for SOT applications (Zhang W. et al., 2016; Shao et al.,

TABLE 1 | Main results for 2D vdW/FM SOT devices.

Material	Fabrication technique	Torques	Resistivity (μΩ cm)	Spin torque conductivity (10^3ħ/2e·Ω^{-1}m^{-1})	Measurement techniques	Author (et al.)
2D semiconductors						
WS_2	CVD	ζ_{FL}/ζ_{DL} = 0.15–0.45	-	-	ST-FMR	Lv Lv et al. (2018)
WSe_2	CVD	-	-	σ_{FL} = 5.52	SHH	Shao Shao et al. (2016)
MoS_2	CVD	ζ_{DL} = 0, ζ_{FL} = 0.14	4,861	σ_{FL} = 2.88	SHH	Shao Shao et al. (2016)
	CVD	ζ_{FL}/ζ_{DL} = 0.19	-	-	ST-FMR	Zhang Zhang et al. (2016b)
2D semimetals						
WTe_2	Exfoliation	$\zeta_{DL,\ in\ plane}$ = 0.029, $\zeta_{DL,\ out\text{-}of\text{-}plane}$ = 0.013, ζ_{FL} = 0.033	385	$\sigma_{DL,\ in\ plane}$ = 8 ± 2, $\sigma_{DL,\ out\text{-}of\text{-}plane}$ = 3.6 ± 0.8	ST-FMR	MacNeill MacNeill et al. (2017b)
	Exfoliation	ζ_{DL} = 0.51	580	σ_{FL} = 9 ± 3 σ_{DL} = 87.9	ST-FMR	Shi Shi et al. (2019)
$MoTe_2$	Exfoliation	$\zeta_{DL,\ in\ plane}$ = 0.032, $\zeta_{DL,\ out\text{-}of\text{-}plane}$ = 0.006, ζ_{FL} = 0.004	550	$\sigma_{DL,\ in\ plane}$ = 5.8, $\sigma_{DL,\ out\text{-}of\text{-}plane}$ = 1.0 σ_{FL} = 0.81	ST-FMR	Stiehl Stiehl et al. (2019a)
	Exfoliation	ζ_{DL} = 0.13–0.35	542	σ_{DL} = 24–64.6	ST-FMR	Liang Liang et al. (2020)
$PtTe_2$	Sputtering	ζ_{DL} = 0.05–0.15,	33–333	σ_{DL} = 20–160	ST-FMR	Xu Xu et al. (2020)
2D metals						
$NbSe_2$	Exfoliation	ζ_{DL} = 0.005–0.013	166.7	σ_{DL} = 3–7.8	ST-FMR	Guimaraes Guimarães et al. (2018)
TaS_2	Sputtering	ζ_{DL} = 0.25	16.9	σ_{DL} = 1,490	ST-FMR/SHH	Husain Husain et al. (2020a)
2D insulator						
$NiPS_3$	Exfoliation	-	10^{17}	σ_{DL} = 60–220, σ_{FL} = 10–17	SHH	Schippers Schippers et al. (2020)
Topological insulators and conventional heavy metals						
Bi_2Se_3	MBE	ζ_{DL} = 2–3.5	1754	σ_{DL} = 110–200, σ_{FL} = 140–160	ST-FMR	Mellnik Mellnik et al. (2014)
Bi_xSe_{1-x}	Sputtering	ζ_{DL} = 8.6–18.6	12821	σ_{DL} = 67–145	ST-FMR/SHH	Mahendra Dc et al. (2018)
Pt	Sputtering	ζ_{DL} = 0.056	20	σ_{DL} = 280	ST-FMR	Liu Liu et al. (2011)
Ta	Sputtering	ζ_{DL} = −0.12	190	σ_{DL} = 63	ST-FMR	Liu Liu et al. (2012b)
W	Sputtering	ζ_{DL} = −0.3	170	σ_{DL} = 176	ST-FMR	Venta de la Venta et al. (2013)

2016; Lv et al., 2018). 2D magnetic materials with simple components, such as CrTe (Wang M. et al., 2020), $FeTe_2$ (Chen et al., 2020) and $CrSe_2$ (Li et al., 2021), have also been successfully prepared by CVD, which provide a good platform for studying the engineering of SOT devices at the 2D scale. The bottlenecks of this method are mainly concentrated in two aspects. The first challenge is the synthesis of complex alloys, like ternary magnets, e.g. Fe_3GeTe_2 (FGT) (Huang et al., 2017; Fei et al., 2018), $Cr_2Ge_2Te_6$ (CGT) (Gong et al., 2017), and $CrSiTe_3$ (Ito et al., 2019), which are mainstream SOT devices based on 2D

magnets. The second challenge concerns the construction of magnetic heterostructures with sharp and ordered interfaces. The preparation of heterostructures by CVD usually requires refuelling or connecting with other equipment, thus the quality of the interface is difficult to guarantee.

Another 2D vdW material preparation method is magnetron sputtering, which is compatible with the current semiconductor industry. The preparation of 2D materials by magnetron sputtering is usually performed in multiple steps while controlling strict growth and annealing conditions. To date, 2D materials for SOT devices prepared by sputtering include $PtTe_2$ (Xu et al., 2020) and TaS_2 (Husain et al., 2020a). Wafer-scale $PtTe_2$ films are prepared through a two-step process, which has been previously used for fabricating $PtSe_2$ (Wang et al., 2015; Yim et al., 2016) and WTe_2 (Zhou et al., 2017). During preparation, Pt thin films are first deposited on Si/SiO_2 wafers by a magnetron sputtering system. They are then transformed into uniform and homogenous $PtTe_2$ thin films by annealing them in tellurium vapour. Similarly, for TaS_2 (Husain et al., 2020a), as-deposited Ta ultra-thin films are transferred to a high vacuum chamber for the plasma-assisted sulfurization process. It is noted that the spin Hall conductivity of $PtTe_2$ and TaS_2 prepared by sputtering are superior to values reported for many other 2D vdW materials, denoting the high-quality of 2D vdW materials prepared by the sputtering method.

In addition to the above three preparation methods, molecular beam epitaxy (MBE) has also attracted considerable attention (Walsh and Hinkle, 2017). MBE offers promising solutions to improve the interface quality of magnetic heterostructures thanks to its high purity solid source materials and ultra-high vacuum growth environment. Recently, heterostructures such as CGT/$(Bi,Sb)_2Te_3$ (Mogi et al., 2018) and FGT/Bi_2Te_3 (Wang H. et al., 2020) with high-quality interfaces have been successfully prepared. Although it has not been widely used for SOT applications yet, it is believed that MBE has its irreplaceable role for 2D SOT devices in the near future.

SOT Devices Based on 2D vdW Material/FM Heterostructures

Extensive 2D Materials including semiconductors, semimetals, metals and insulators have been used as the spin source layer, among which TMDs draw the most attention for high SOT efficiency and the out-of-plane damping-like torque induced by the broken symmetry. Following, we review the main results on 2D vdW material/FM heterostructures for SOT applications, as is listed in **Table 1**.

2D Semiconductor/FM

Current induced SOT was first observed in monolayer 2D vdW semiconductor MoS_2/Py by Zhang et al. using spin-torque ferromagnetic resonance (ST-FMR) (Zhang W. et al., 2016). Both out-of-plane field-like torque ζ_{FL} and in-plane damping-like torque ζ_{DL} are observed, and a torque ratio $\zeta_{FL}/\zeta_{DL} = 0.19 \pm 0.01$ was quantified by the lineshape analysis, indicating the potential of 2D TMDs for the use of interfacial spin-orbitronics applications. Later on, Shao et al. examined the SOT in monolayer MoS_2 and WSe_2 coupled with CoFeB by another measurement technique, second-harmonic Hall (SHH) (Shao et al., 2016). In contrast to the results by Zhang and co-workers, Shao et al. detected only the out-of-plane field-like torque ζ_{FL}, and there is no evidence of damping-like torques in both MoS_2/CoFeB and WSe_2/CoFeB bilayers. The torques are temperature-dependent, and the corresponding spin Hall conductivity σ_{FL} is equal to 2.88×10^3 $(\hbar/2e)$ $(\Omega m)^{-1}$ and 5.52×10^3 $(\hbar/2e)$ $(\Omega m)^{-1}$ at room temperature for MoS_2 and WSe_2 respectively. They attributed the SOTs to the Rashba-Edelstein effect. Furthermore, Lv et al. demonstrated that the SOT ratio between the field-like and damping-like torques can be controlled by applying the back-gate voltage in WS_2/Py heterostructures (Lv et al., 2018), as shown in **Figure 2A,B** The effective modulation of SOTs by electrical voltage opens a new door for developing and applying SOT devices in data storage and processing. It is noted that although the spin-charge conservation efficiency in 2D vdW semiconductors is comparable to conventional HMs, their resistivity is several orders of magnitude higher than that of HMs, leading to most of the current flowing in the FM layer and hence much power consumption. In order to overcome this limitation and improve the energy efficiency of SOT devices, more and more studies are focused on 2D semimetals with large conductivity, as will be introduced as follow.

2D Semimetal/FM

Pioneering works on 2D semimetals for SOT applications are performed by MacNeill et al. on WTe_2 (MacNeill et al., 2017a), a Weyl semimetal that features an open Fermi arc with strong SOC and spin–momentum locking effect. Notably, the surface crystal structure of WTe_2 has only one mirror plane. In their study, the in-plane damping-like torque ($\zeta_{DL,\ in\text{-}plane} = 0.029$) and the out-of-plane field-like torque ($\zeta_{FL} = 0.033$) are both detected by ST-FMR, and the corresponding spin-torque conductivities are 8×10^3 $(\hbar/2e)$ $(\Omega m)^{-1}$ and 9×10^3 $(\hbar/2e)$ $(\Omega m)^{-1}$ respectively. Particularly, when an electric current is applied along the low-symmetry axis of WTe_2, an unconventional out-of-plane damping-like torque ($\zeta_{DL,\ out\text{-}of\text{-}plane} = 0.013$, $\sigma_{DL,\ out\text{-}of\text{-}plane} = 3.6 \times 10^3$ $(\hbar/2e)$ $(\Omega m)^{-1}$) is applied on the adjacent Py film, as is shown in **Figure 2C,D** The torques were further confirmed by the SHH technique (MacNeill et al., 2017b) and remain large down to WTe_2 monolayer, providing a new strategy for optimizing the manipulation of magnetisation in SOT devices with perpendicular magnetic anisotropy (PMA). Recently, a step forward has been made using SOTs in WTe_2/Py heterostructures to switch magnetization (Shi et al., 2019), where the damping-like SOT was as large as 0.51, and the switching current density is in the order of 10^5 A/cm^2. The power consumption required to switch the magnetization in WTe_2/Py is much lower than average values in Bi_2Se_3/Py or Pt/Py.

Similar studies were also performed by Stiehl et al. on another 2D semimetal 1*T*'-$MoTe_2$ (Stiehl et al., 2019a). Unlike WTe_2, 1*T*'-$MoTe_2$ retains a bulk inversion symmetry while the surface symmetry is limited to just one mirror plane. By ST-FMR, the

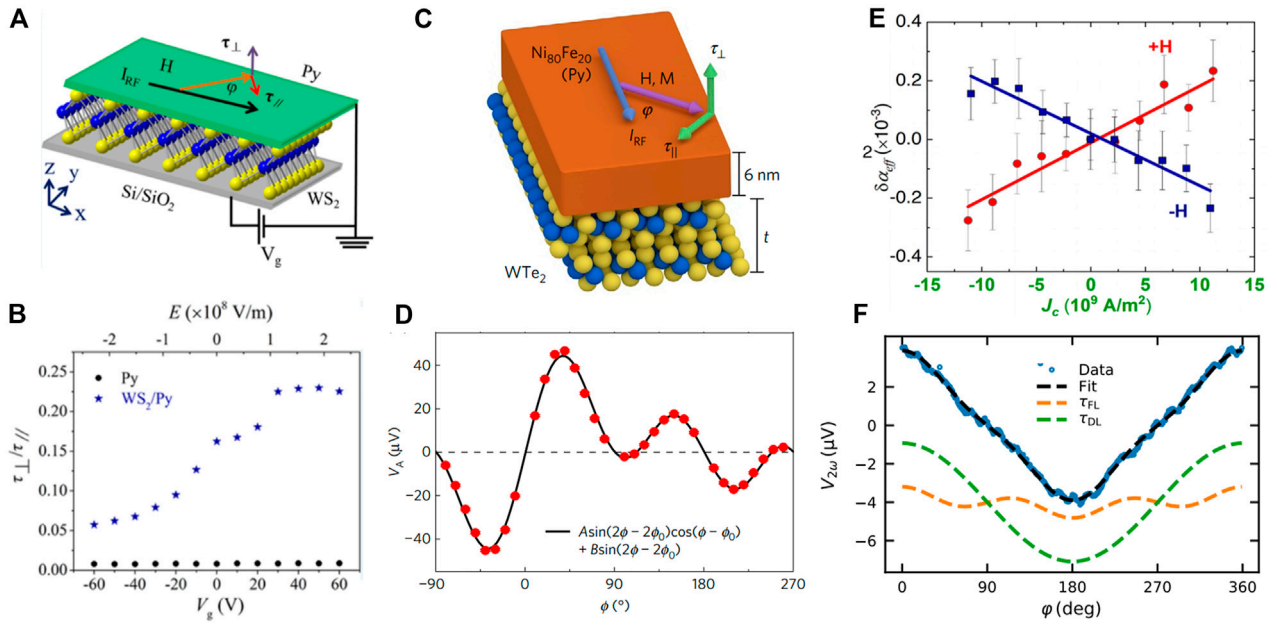

FIGURE 2 | 2D vdW/FM SOT devices: **(A)** Schematic of the WS_2/Py heterostructure (Lv et al., 2018). **(B)** The ratio between the out-of-plane field-like torque and the in-plane damping-like torque controlled by the gate voltage. **(C)** Schematic of the WTe_2/Py heterostructure (MacNeill et al., 2017a). **(D)** Antisymmetric components of the ST-FMR spectra detected at a magnetic field with different directions when the electric current is applied parallel to the low-symmetry crystal axis. **(E)** DC-induced changes of effective damping in the TaS_2/Py heterostructure for positive and negative field directions (Husain et al., 2020a). **(F)** Harmonic Hall voltage detected at a magnetic field of 34 mT with different angles. Contributions of the damping-like SOT and the field-like SOT are extracted by numerical fitting, which are shown by green and orange dashed lines (Schippers et al., 2020).

average in-plane damping-like torque conductivity is extracted as 5.8×10^3 $(\hbar/2e)$ $(\Omega m)^{-1}$, and the field-like torque conductivity is 0.8×10^3 $(\hbar/2e)$ $(\Omega m)^{-1}$. When the current is perpendicular to the single mirror plane, the spin conductivity of the out-of-plane damping-like torque induced by interfacial inversion symmetry breaking of $MoTe_2$ is 1.0×10^3 $(\hbar/2e)$ $(\Omega m)^{-1}$, which is about 1/3 of that of WTe_2 (MacNeill et al., 2017a). Recently, a large spin Hall angle of 0.32 accompanied by a long spin-diffusion length of 2.2 μm in $MoTe_2$ was reported by Song et al. (2020), identifying $MoTe_2$ as an excellent candidate for simultaneous spin generation, transport and detection. More recently, magnetization switching was realized by Liang and coauthors in $MoTe_2$/Py (Liang et al., 2020), and the critical current density is in the order of 10^5 A/cm^2, which is similar to that of WTe_2/Py.

To explore materials with more significant spin-torque conductivity, Xu et al. examined the type-II Dirac semimetal, $PtTe_2$ (Xu et al., 2020), whose resistivity is lower than WTe_2 and the nontrivial topological invariant gives rise to topological surface states (TSSs) with spin-momentum locking. They found that the SOT conductivity of $PtTe_2$ is as large as 160×10^3 $(\hbar/2e)$ $(\Omega m)^{-1}$, which is comparable to that of the best-performing heavy metals and topological insulators. Additionally, Xu and coauthors realized switching of perpendicular magnetization in $PtTe_2$/Au/CoTb devices with the critical current density in the order of 10^6~10^7 A/m^2. It is noted that although the SOT conductivity of $PtTe_2$ is larger than WTe_2 and $MoTe_2$, the critical current density for magnetization switching in $PtTe_2$ shows an opposite trend. Such a discrepancy between the SOT conductivity and the critical switching current density have also been reported by Zhu et al. (2021), and the physics at work might depend on the saturation magnetization, the Dzyaloshinskii-Moriya interaction, and the magnetic damping, which require future efforts to understand. Recently, another topological semimetal, Ta_3As, was predicted to has a large SOT conductivity around 150×10^3 $(\hbar/2e)$ $(\Omega m)^{-1}$ (Hou et al., 2021). This prediction promotes further research on SOT devices based on 2D semimetals with topological and superconductivity properties.

2D Metal/FM

Compared with 2D semiconductors and semimetals, there are fewer kinds of 2D metallic materials, and only a tiny part of them are used for SOTapplications. Although by far there are only a few of studies reported, 2D metals hold the most potential for SOT application, due to their extremely low resistivities. The first research of SOTs generated by a metallic 2D vdW material is performed on $NbSe_2$ (Guimarães et al., 2018), where an in-plane damping-like torque with torque conductivity $\sigma_{DL} \approx 3 \times 10^3$ $(\hbar/2e)$ $(\Omega m)^{-1}$ is detected by ST-FMR. Besides, an in-plane field-like torque is observed and varies from sample to sample, consisting of the symmetry breaking by a uniaxial strain that might result from device fabrication. Another metallic 2D vdW material used for SOT applications is TaS_2 (Husain et al., 2020a), which exhibits to date the lowest room-temperature resistivity (≈16.9 μΩ cm) among metallic TMDs (**Figure 2E**). The SOTs were measured by using both ST-FMR and SHH, and the damping-like SOT

conductivity is found to be 1,490 × 10^3 ($\hbar/2e$) $(\Omega m)^{-1}$, which is superior to values reported on other 2D vdW materials.

2D Insulator/FM

During the development of SOT devices, 2D insulators have received the least attention than other material counterparts. To date, only one experimental study was reported on antiferromagnetic insulator NiPS3/Py bilayers (Hidding and Guimarães, 2020), where an ample in-plane damping-like torque was induced at the interface. **Figure 2F** shows the result detected from the angular dependent SHH measurement, the most immense value of the damping-like SOT conductivity they detected at room temperature is 220 × 10^3 ($\hbar/2e$) $(\Omega m)^{-1}$, which is larger than most of the values reported in other 2D vdW materials. Moreover, temperature-dependent measurements revealed an increased SOT with a decreasing temperature below the Néel temperature of $NiPS_3$ ($T_N \approx 170$ K), suggesting a possible effect of the magnetic ordering on SOTs.

SOT Devices Based on 2D vdW Magnet/HM Heterostructures

In the past 4 years, notable examples of magnetic order have been observed in 2D vdW materials, which bring new prospects for spintronic devices. Manipulation of the magnetization in 2D magnets via SOTs is a new branch of spin-orbitronics, a feasible scheme of which is combining the 2D magnet with heavy metal film.

FGT is currently one of the most attractive vdW layered ferromagnets due to its stable PMA and high Curie temperature. SOTs in FGT/Pt heterostructures have been studied by Wang et al. (2019) and Alghamdi et al. (2019). Similar results show that the lower-bound damping-like torque in FGT/Pt bilayer is about 0.1, and the critical current density for magnetization switching is in the order of 10^7 A/cm^2, as shown in **Figure 3A–C** Most recently, by further improving the quality of the interface, the minimum of SOT efficiency in FGT/Pt is determined to be 0.18 (Zhang et al., 2021), which is higher than that in previous studies, and comparable to the values for the Pt/Co and Pt/CoFeB bilayers (Pai et al., 2015; Nguyen et al., 2016), indicating the importance of the high-quality interface for SOT devices.

Apart from the metallic 2D magnet FGT, investigations on SOTs in semiconducting 2D ferromagnets were also reperted recently. Ostwal et al. (2020) and Gupta et al. (2020) separately studied the current induced switching of a ferromagnetic semiconductor CGT. It was found that a current with a density as low as 10^5A cm^{-2} is sufficient to switch the out-of-plane magnetization of CGT in CGT/Ta heterostructure, as is shown in **Figure 3D–F** This current density is about two orders of magnitude lower than those required for switching metallic ferromagnets such as CoFeB (Zhang C. et al., 2016), Py (Liu et al., 2011) and FGT (Alghamdi et al., 2019; Wang et al., 2019), benefiting from the negligible shunting effect of the electrical current in such structures. Recently, Su et al. demenstrated the current dependent magnetoresistance (MR) of CrI_3 by combining with Pt (Su et al., 2020), indicating the potential effect of SOTs on CrI_3 induced by SHE in Pt.

Evidence of SOTs on 2D ferromagnets are also observed in a 2D ferromagnetic insulator Co-Doped MoS_2 (Huang M. et al., 2020) by measuring the spin Hall magnetoresistance (SMR) in Co-Doped MoS_2/Ta bilayer. We believe that the emerging family of vdW magnets remarkably extend the material choices and construct new building blocks for spintronic applications.

SOT Devices Based on All-vdW Heterostructures

Because of the vdW nature of 2D materials, an atomically sharp interface can be achieved in an all-vdW heterostructure, which is crucially important for a high SOT efficiency. SOT devices based on all-vdW heterostructures was first put forward by Dolui et al. (2020). They theoretically predicted that the field-free magnetization switching can be induced by SOTs in a bilayer-CrI_3/monolayer-$TaSe_2$ vdW heterostructure, which has attracted great attentions in this field. Another theoretical work focused on CGT/ graphene/WS_2 vdW heterostructure was reported by Zollner et al. (2020b). Using first principles combined with quantum transport calculations, they found that a damping-like SOT is able to be generated by skew scattering, and the ratio of field-like and damiping-like components of SOTs can be tuned by two orders of magnitude via gate voltage. In a single device consisting of a bilayer graphene sandwiched by a CGT and a monolayer WS_2, it is able not only to generate, but also to swap the two spin interactions of exchange and spin-orbit coupling (Zollner et al., 2020a). These pioneering theoretical researches provide bases for further experiments and applications of all-van der Waals SOT devices.

Experimental studies on SOTs in all-vdW heterostructures were preliminarily explored very recently. A significant SOT efficiency of 4.6 along with a dramatically high SOT conductivity of 1,035 × 10^3 ($\hbar/2e$) $(\Omega m)^{-1}$ was reported in WTe_2/FGT bilayers (Shin et al., 2021). The switching current density is about 3.9 × 10^6 A/cm^2. Such an extraordinary value of SOT conductivity may benefit from the clean interface between WTe_2 and FGT in their devices. Utilizing the out-of-plane damping-like SOT induced in WTe_2 with low-crystal symmetry, Kao et al. (2020) achieved the field-free deterministic magnetic switching of FGT, highlighting the superiority of 2D vdW heterostructures in energy-efficient magnetization control in SOT-based spintronics.

PERFORMANCE MODULATION OF CONVENTIONAL SOT DEVICES BY 2D VDW MATERIALS

In addition to the main effect in the above structures, 2D vdW materials are also used to assist in improving the SOT efficiency in conventional HM/FM heterostructures.

Recently, the hybrid between 2D vdW materials with HM/FM films has proved to be a good candidate for energy-efficient SOT devices (Xie et al., 2019; Debashis et al., 2020; Lv et al., 2021). It was experimentally demonstrated that the SOT efficiency in Pt/$(Co/Ni)_2$ was 17 times enhanced by MoS_2 underlayer (Xie et al.,

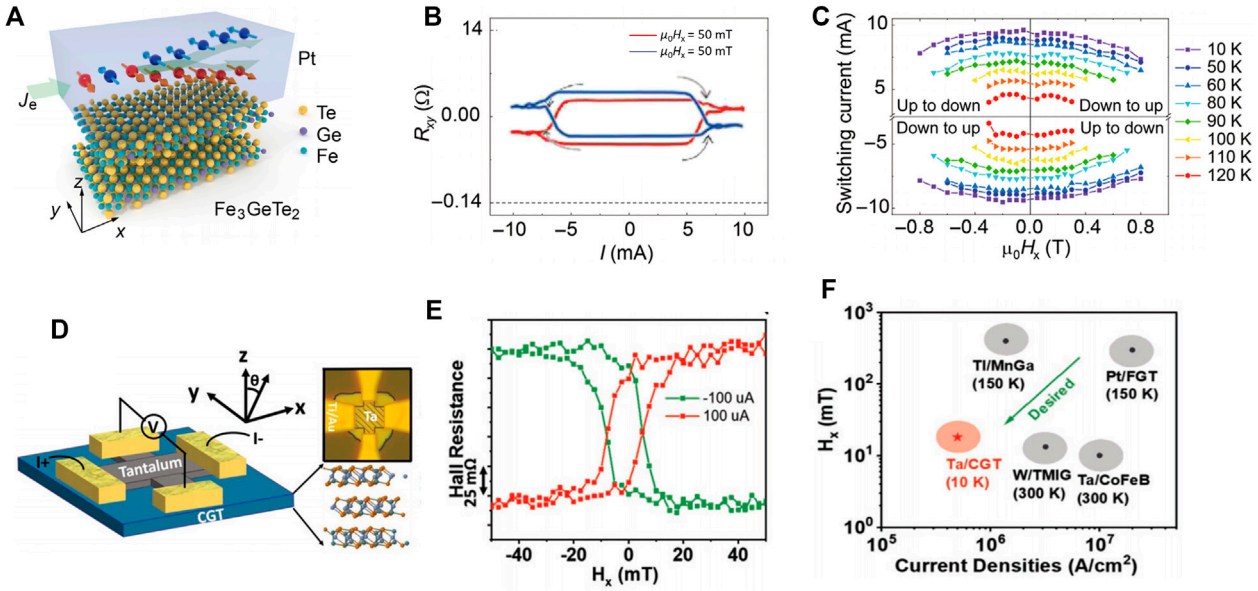

FIGURE 3 | 2D magnet/HM SOT devices: **(A)** Schematic of the FGT/Pt heterostructure (Wang et al., 2019). **(B)** SOT-driven magnetization switching for in-plane magnetic fields of 50 mT and −50 mT on the FGT/Pt bilayer devices at 100 K. **(C)** Critical switching current as a function of the in-plane magnetic field at different temperatures. The applied current of 1 mA corresponds to a current density of 1.85×10^{10} A/m^2 in the Pt layer. **(D)** Schematic of the CGT/Ta heterostructure (Ostwal et al., 2020). **(E)** Field assisted SOT-driven magnetization switching with currents of 100 μA and −100 μA at 4 K. **(F)** Assistant fields and current densities needed for SOT-driven switching of previous studies compared to the results obtained from CGT/ Pt.

2019), but the underlying mechanisms need to be further investigated. A similar phenomenon was also observed in Ta/CoFeB with a monolayer WSe_2 inserted as an underlayer (Debashis et al., 2020). In that work, the SOT efficiency is enhanced by more than 25 times due to the potential spin absorption at the Ta/WSe_2 interface. Besides, as an inset layer between FM and HM, it is expected that the 2D vdW materials may work for interfacial engineering. Evidence can be observed in several relevant studies reported in the recent past (Dastgeer et al., 2019; Lee et al., 2020; Lee et al., 2021a; Lee et al., 2021b; Novakov et al., 2021). Novakov and coauthors observed enhanced spin torques from the Rashba spin current in heterostructures of Py and WSe_2, indicating that the insertion of low layer WSe_2 can be used as an interlayer "scattering promoter" in heterostructure interfaces without quenching the original polarization (Novakov et al., 2021). Lee et al. investigated the longitudinal spin Seebeck effect in magnetic heterostructures with vdW interface, and found that the spin fluctuation in inserted WSe_2 (Lee et al., 2021a) or MoS_2 (Lee et al., 2020; Lee et al., 2021b) can amplify the spin current transmission between HM and FM films. Further works in this area are worthy to be carried on.

CONCLUSION AND FUTURE PERSPECTIVE

Over the last decade, 2D vdW materials have brought fresh stimuli to SOT devices. The large family of vdW and numerous combinations of vdW heterostructures will widely extend the material choices and bring new opportunities in SOT devices in the future. Numerous advantages make vdW materials promising candidates for emerging applications in spin-orbitronics. Based on this review, we suggest the following three important research directions in this field.

The first direction is the preparing and interface engineering of novel 2D SOT devices. The quality of the material and the interface condition of the heterostructure play decisive roles in the performance of SOT devices. At present, there are still difficulties in preparing large-area 2D vdW materials with high quality and controllable thickness, thus interfacial engineering remains a challenge for most of the 2D SOT devices. Innovative exfoliation techniques such as the vacuum exfoliation approach (Zhang et al., 2021) need to be developed. CVD methods could be further optimized, especially in the synthesis of large-scaled complex alloys. Notably, we look forward to the employment of an *in-situ* growth strategy for 2D vdW magnetic heterostructures for SOT applications, which holds unique advantages to the quality of the material and the interface.

The second direction is the performance modulation of SOT devices. Pioneer works in this aspect were performed by Lv et al. (2018), and affective modulation of SOTs by electrical voltage is successfully realised, suggesting the feasibility of the idea of modulated SOT performance. In recent years, it has been reported that the rich magneto-electric properties of 2D vdW materials can be regulated by electric field (Deng et al., 2018; Huang et al., 2018; Jiang et al., 2018; Park et al., 2020; Zhuo et al., 2021), light (Liu et al., 2020), and strain (Wang Y. et al., 2020; Hu et al., 2020; Zhuo et al., 2021). Therefore, it is expected that the performance of 2D SOT devices can be manipulated by controlling multi-field conditions.

The third direction is the field-free magnetization switching using 2D vdW materials with low crystal symmetries. The crystal symmetry induced out-of-plane damping-like SOT in some 2D vdW materials suggests a strategy for field-free switching of perpendicularly magnetize system (Liu et al., 2021). To date, various approaches for field-free SOT-induced magnetization switching of PMA systems have been proposed and demonstrated. Examples include using a wedgy oxide capping layer (Yu et al., 2014), a polarized ferroelectric substrate (Cai et al., 2017), lateral SOT (Cao et al., 2020a), introducing an interlayer coupling (Fukami et al., 2016; Lau et al., 2016). Compared with these previous methods, 2D vdW materials broaden the scope of material engineering for conventional SOT devices. Moreover, SOT driven magnetization switching in 2D vdW ferromagnets fuels the low-dimensional spintronic applications, but further work is still needed to push the 2D vdW ferromagnet down to the monolayer limit.

AUTHOR CONTRIBUTIONS

YZ and QC conceived and initiated this project. MT and with the help received from QC and MJ wrote the paper. YZ, WJ and JL were instrumental in making the table and figures. ZH and ZZ helped in drafting the content and correction of the review. All authors contributed to the article and approved the submitted version.

FUNDING

The authors would like to acknowledge the financial support from the National Key Research and Development Program of China, China (Grant No. 2017YFA0204800), and the National Natural Science Foundation of China (Grant Nos. 52071079, 51732010).

REFERENCES

Alghamdi, M., Lohmann, M., Li, J., Jothi, P. R., Shao, Q., Aldosary, M., et al. (2019). Highly Efficient Spin-Orbit Torque and Switching of Layered Ferromagnet Fe3GeTe2. *Nano Lett.* 19, 4400–4405. doi:10.1021/acs.nanolett.9b01043

Avci, C. O., Garello, K., Nistor, C., Godey, S., Ballesteros, B., Mugarza, A., et al. (2014). Fieldlike and Antidamping Spin-Orbit Torques in As-Grown and Annealed Ta/CoFeB/MgO Layers. *Phys. Rev. B.* 89, 214419. doi:10.1103/PhysRevB.89.214419

Brataas, A., Kent, A. D., and Ohno, H. (2012). Current-induced Torques in Magnetic Materials. *Nat. Mater.* 11, 372–381. doi:10.1038/nmat3311

Cai, K., Yang, M., Ju, H., Wang, S., Ji, Y., Li, B., et al. (2017). Electric Field Control of Deterministic Current-Induced Magnetization Switching in a Hybrid Ferromagnetic/ferroelectric Structure. *Nat. Mater.* 16, 712–716. doi:10.1038/nmat4886

Cao, Y., Sheng, Y., Edmonds, K. W., Ji, Y., Zheng, H., and Wang, K. (2020a). Deterministic Magnetization Switching Using Lateral Spin-Orbit Torque. *Adv. Mater.* 32, e1907929. doi:10.1002/adma.201907929

Cao, Y., Xing, G., Lin, H., Zhang, N., Zheng, H., and Wang, K. (2020b). Prospect of Spin-Orbitronic Devices and Their Applications. *iScience* 23, 101614. doi:10.1016/j.isci.2020.101614

Chen, S., Liu, H., Chen, F., Zhou, K., and Xue, Y. (2020). Synthesis, Transfer, and Properties of Layered FeTe2 Nanocrystals. *ACS Nano* 14, 11473–11481. doi:10.1021/acsnano.0c03863

Dastgeer, G., Shehzad, M. A., and Eom, J. (2019). Distinct Detection of Thermally Induced Spin Voltage in Pt/WS2/Ni81Fe19 by the Inverse Spin Hall Effect. *ACS Appl. Mater. Inter.* 11, 48533–48539. doi:10.1021/acsami.9b16476

Dc, M., Grassi, R., Chen, J.-Y., Jamali, M., Reifsnyder Hickey, D., Zhang, D., et al. (2018). Room-temperature High Spin-Orbit Torque Due to Quantum Confinement in Sputtered BixSe(1-X) Films. *Nat. Mater.* 17, 800–807. doi:10.1038/s41563-018-0136-z

de la Venta, J., Wang, S., Ramirez, J. G., and Schuller, I. K. (2013). Control of Magnetism across Metal to Insulator Transitions. *Appl. Phys. Lett.* 102, 122404. doi:10.1063/1.4798293

Debashis, P., Hung, T. Y. T., and Chen, Z. (2020). Monolayer WSe2 Induced Giant Enhancement in the Spin Hall Efficiency of Tantalum. *Npj 2d Mater. Appl.* 4, 18. doi:10.1038/s41699-020-0153-z

Deng, Y., Yu, Y., Song, Y., Zhang, J., Wang, N. Z., Sun, Z., et al. (2018). Gate-tunable Room-Temperature Ferromagnetism in Two-Dimensional Fe3GeTe2. *Nature* 563, 94–99. doi:10.1038/s41586-018-0626-9

Desai, S. B., Madhvapathy, S. R., Amani, M., Kiriya, D., Hettick, M., Tosun, M., et al. (2016). Gold-Mediated Exfoliation of Ultralarge Optoelectronically-Perfect Monolayers. *Adv. Mater.* 28, 4053–4058. doi:10.1002/adma.201506171

Dolui, K., Petrović, M. D., Zollner, K., Plecháč, P., Fabian, J., and Nikolić, B. K. (2020). Proximity Spin-Orbit Torque on a Two-Dimensional Magnet within van der Waals Heterostructure: Current-Driven Antiferromagnet-to-Ferromagnet Reversible Nonequilibrium Phase Transition in Bilayer CrI3. *Nano Lett.* 20, 2288–2295. doi:10.1021/acs.nanolett.9b04556

Dresselhaus, G. (1955). Spin-Orbit Coupling Effects in Zinc Blende Structures. *Phys. Rev.* 100, 580–586. doi:10.1103/PhysRev.100.580

Dyakonov, M. I., and Perel, V. I. (1971). Current-induced Spin Orientation of Electrons in Semiconductors. *Phys. Lett. A.* 35, 459–460. doi:10.1016/0375-9601(71)90196-4

Edelstein, V. M. (1990). Spin Polarization of Conduction Electrons Induced by Electric Current in Two-Dimensional Asymmetric Electron Systems. *Solid State. Commun.* 73, 233–235. doi:10.1016/0038-1098(90)90963-C

Fei, Z., Huang, B., Malinowski, P., Wang, W., Song, T., Sanchez, J., et al. (2018). Two-dimensional Itinerant Ferromagnetism in Atomically Thin Fe3GeTe2. *Nat. Mater.* 17, 778–782. doi:10.1038/s41563-018-0149-7

Fukami, S., Zhang, C., Duttagupta, S., Kurenkov, A., and Ohno, H. (2016). Magnetization Switching by Spin-Orbit Torque in an Antiferromagnet-Ferromagnet Bilayer System. *Nat. Mater.* 15, 535–541. doi:10.1038/nmat4566

Gong, C., Li, L., Li, Z., Ji, H., Stern, A., Xia, Y., et al. (2017). Discovery of intrinsic ferromagnetism in two-dimensional van der Waals crystals. *Nature* 546, 265–269. doi:10.1038/nature22060

Gong, C., and Zhang, X. (2019). Two-dimensional Magnetic Crystals and Emergent Heterostructure Devices. *Science* 363, 363eaav4450. doi:10.1126/science.aav4450

Grytsyuk, S., Belabbes, A., Haney, P. M., Lee, H.-W., Lee, K.-J., Stiles, M. D., et al. (2016). K-Asymmetric Spin Splitting at the Interface between Transition Metal Ferromagnets and Heavy Metals. *Phys. Rev. B.* 93, 174421. doi:10.1103/PhysRevB.93.174421

Guimarães, M. H. D., Stiehl, G. M., MacNeill, D., Reynolds, N. D., and Ralph, D. C. (2018). Spin-Orbit Torques in NbSe2/Permalloy Bilayers. *Nano Lett.* 18, 1311–1316. doi:10.1021/acs.nanolett.7b04993

Gupta, V., Cham, T. M., Stiehl, G. M., Bose, A., Mittelstaedt, J. A., Kang, K., et al. (2020). Manipulation of the van der Waals Magnet Cr2Ge2Te6 by Spin-Orbit Torques. *Nano Lett.* 20, 7482–7488. doi:10.1021/acs.nanolett.0c02965

Han, X., Wang, X., Wan, C., Yu, G., and Lv, X. (2021). Spin-orbit Torques: Materials, Physics, and Devices. *Appl. Phys. Lett.* 118, 120502. doi:10.1063/5.0039147

He, Z., Zhang, Y., Angizi, S., Gong, B., and Fan, D. (2018). Exploring a SOT-MRAM Based In-Memory Computing for Data Processing. *IEEE Trans. Multi-scale Comp. Syst.* 4, 676–685. doi:10.1109/TMSCS.2018.2836967

Hidding, J., and Guimarães, M. H. D. (2020). Spin-Orbit Torques in Transition Metal Dichalcogenide/Ferromagnet Heterostructures. *Front. Mater.* 7, 594771. doi:10.3389/fmats.2020.594771

Hirsch, J. E. (1999). Spin Hall Effect. *Phys. Rev. Lett.* 83, 1834–1837. doi:10.1103/PhysRevLett.83.1834

Hou, W., Liu, J., Zuo, X., Xu, J., Zhang, X., Liu, D., et al. (2021). Prediction of Crossing Nodal-Lines and Large Intrinsic Spin Hall Conductivity in

Topological Dirac Semimetal Ta3As Family. *Npj Comput. Mater.* 7, 37. doi:10.1038/s41524-021-00504-w

Hu, X., Zhao, Y., Shen, X., Krasheninnikov, A. V., Chen, Z., and Sun, L. (2020). Enhanced Ferromagnetism and Tunable Magnetism in Fe3GeTe2 Monolayer by Strain Engineering. *ACS Appl. Mater. Inter.* 12, 26367–26373. doi:10.1021/acsami.0c05530

Huang, B., Clark, G., Klein, D. R., MacNeill, D., Navarro-Moratalla, E., Seyler, K. L., et al. (2018). Electrical Control of 2D Magnetism in Bilayer CrI3. *Nat. Nanotech.* 13, 544–548. doi:10.1038/s41565-018-0121-3

Huang, B., Clark, G., Navarro-Moratalla, E., Klein, D. R., Cheng, R., Seyler, K. L., et al. (2017). Layer-dependent ferromagnetism in a van der Waals crystal down to the monolayer limit. *Nature* 546, 270–273. doi:10.1038/nature22391

Huang, M., Xiang, J., Feng, C., Huang, H., Liu, P., Wu, Y., et al. (2020a). Direct Evidence of Spin Transfer Torque on Two-Dimensional Cobalt-Doped MoS2 Ferromagnetic Material. *ACS Appl. Electron. Mater.* 2, 1497–1504. doi:10.1021/acsaelm.0c00384

Huang, Y., Pan, Y.-H., Yang, R., Bao, L.-H., Meng, L., Luo, H.-L., et al. (2020b). Universal Mechanical Exfoliation of Large-Area 2D Crystals. *Nat. Commun.* 11, 2453. doi:10.1038/s41467-020-16266-w

Husain, S., Chen, X., Gupta, R., Behera, N., Kumar, P., Edvinsson, T., et al. (2020a). Large Damping-like Spin-Orbit Torque in a 2D Conductive 1T-TaS2 Monolayer. *Nano Lett.* 20, 6372–6380. doi:10.1021/acs.nanolett.0c01955

Husain, S., Gupta, R., Kumar, A., Kumar, P., Behera, N., Brucas, R., et al. (2020b). Emergence of Spin-Orbit Torques in 2D Transition Metal Dichalcogenides: A Status Update. *Appl. Phys. Rev.* 7, 041312. doi:10.1063/5.0025318

Ito, N., Kikkawa, T., Barker, J., Hirobe, D., Shiomi, Y., and Saitoh, E. (2019). Spin Seebeck Effect in the Layered Ferromagnetic Insulators CrSiTe3 and CrGeTe3. *Phys. Rev. B.* 100, 060402. doi:10.1103/PhysRevB.100.060402

Jiang, S., Shan, J., and Mak, K. F. (2018). Electric-field switching of two-dimensional van der Waals magnets. *Nat. Mater.* 17, 406–410. doi:10.1038/s41563-018-0040-6

Kao, I.-H., Muzzio, R., Zhang, H., Zhu, M., Gobbo, J., Weber, D., et al. (2020). *Field-free Deterministic Switching of a Perpendicularly Polarized Magnet Using Unconventional Spin-Orbit Torques in WTe2*. 2012.12388. arXiv[Preprint]. Available at: http://arxiv.org/abs/2012.12388.

Kato, Y. K., Myers, R. C., Gossard, A. C., and Awschalom, D. D. (2004). Observation of the Spin Hall Effect in Semiconductors. *Science* 306, 1910–1913. doi:10.1126/science.1105514

Koo, H. C., Kim, S. B., Kim, H., Park, T. E., Choi, J. W., Kim, K. W., et al. (2020). Rashba Effect in Functional Spintronic Devices. *Adv. Mater.* 32, 2002117–2002119. doi:10.1002/adma.202002117

Kurenkov, A., DuttaGupta, S., Zhang, C., Fukami, S., Horio, Y., and Ohno, H. (2019). Artificial Neuron and Synapse Realized in an Antiferromagnet/Ferromagnet Heterostructure Using Dynamics of Spin-Orbit Torque Switching. *Adv. Mater.* 31, 1900636. doi:10.1002/adma.201900636

Lau, Y.-C., Betto, D., Rode, K., Coey, J. M. D., and Stamenov, P. (2016). Spin-orbit Torque Switching without an External Field Using Interlayer Exchange Coupling. *Nat. Nanotech.* 11, 758–762. doi:10.1038/nnano.2016.84

Lee, W.-Y., Kang, M.-S., Kim, G.-S., Park, N.-W., Choi, K.-Y., Le, C. T., et al. (2021a). Role of Ferromagnetic Monolayer WSe2 Flakes in the Pt/Y3Fe5O12 Bilayer Structure in the Longitudinal Spin Seebeck Effect. *ACS Appl. Mater. Inter.* 13, 15783–15790. doi:10.1021/acsami.0c22345

Lee, W.-Y., Park, N.-W., Kang, M.-S., Kim, G.-S., Jang, H. W., Saitoh, E., et al. (2020). Surface Coverage Dependence of Spin-To-Charge Current across Pt/MoS2/Y3Fe5O12 Layers via Longitudinal Spin Seebeck Effect. *J. Phys. Chem. Lett.* 11, 5338–5344. doi:10.1021/acs.jpclett.0c01502

Lee, W.-Y., Park, N.-W., Kim, G.-S., Kang, M.-S., Choi, J. W., Choi, K.-Y., et al. (2021b). Enhanced Spin Seebeck Thermopower in Pt/Holey MoS2/Y3Fe5O12 Hybrid Structure. *Nano Lett.* 21, 189–196. doi:10.1021/acs.nanolett.0c03499

Levy, P. M., Yang, H., Chshiev, M., and Fert, A. (2013). Spin Hall Effect Induced by Bi Impurities in Cu: Skew Scattering and Side-Jump. *Phys. Rev. B.* 88, 214432. doi:10.1103/PhysRevB.88.214432

Li, B., Wan, Z., Wang, C., Chen, P., Huang, B., Cheng, X., et al. (2021). Van der Waals epitaxial growth of air-stable CrSe2 nanosheets with thickness-tunable magnetic order. *Nat. Mater.* 20, 818–825. doi:10.1038/s41563-021-00927-2

Liang, S., Shi, S., Hsu, C. H., Cai, K., Wang, Y., He, P., et al. (2020). Spin-Orbit Torque Magnetization Switching in MoTe 2/Permalloy Heterostructures. *Adv. Mater.* 32, 2002799. doi:10.1002/adma.202002799

Liu, B., Liu, S., Yang, L., Chen, Z., Zhang, E., Li, Z., et al. (2020). Light-Tunable Ferromagnetism in Atomically Thin Fe3GeTe2 Driven by Femtosecond Laser Pulse. *Phys. Rev. Lett.* 125, 267205. doi:10.1103/physrevlett.125.267205

Liu, L., Lee, O. J., Gudmundsen, T. J., Ralph, D. C., and Buhrman, R. A. (2012a). Current-Induced Switching of Perpendicularly Magnetized Magnetic Layers Using Spin Torque from the Spin Hall Effect. *Phys. Rev. Lett.* 109, 096602. doi:10.1103/PhysRevLett.109.096602

Liu, L., Moriyama, T., Ralph, D. C., and Buhrman, R. A. (2011). Spin-torque Ferromagnetic Resonance Induced by the Spin Hall Effect. *Phys. Rev. Lett.* 106, 036601. doi:10.1103/PhysRevLett.106.036601

Liu, L., Pai, C.-F., Li, Y., Tseng, H. W., Ralph, D. C., and Buhrman, R. A. (2012b). Spin-Torque Switching with the Giant Spin Hall Effect of Tantalum. *Science* 336, 555–558. doi:10.1126/science.1218197

Liu, L., Zhou, C., Shu, X., Li, C., Zhao, T., Lin, W., et al. (2021). Symmetry-dependent Field-free Switching of Perpendicular Magnetization. *Nat. Nanotechnol.* 16, 277–282. doi:10.1038/s41565-020-00826-8

Liu, Y., and Shao, Q. (2020). Two-Dimensional Materials for Energy-Efficient Spin-Orbit Torque Devices. *ACS Nano.* 14, 9389–9407. doi:10.1021/acsnano.0c04403

Lv, W., Jia, Z., Wang, B., Lu, Y., Luo, X., Zhang, B., et al. (2018). Electric-Field Control of Spin-Orbit Torques in WS2/Permalloy Bilayers. *ACS Appl. Mater. Inter.* 10, 2843–2849. doi:10.1021/acsami.7b16919

Lv, W., Xue, H., Cai, J., Chen, Q., Zhang, B., Zhang, Z., et al. (2021). Enhancement of Spin-Orbit Torque in WTe2/perpendicular Magnetic Anisotropy Heterostructures. *Appl. Phys. Lett.* 118, 052406. doi:10.1063/5.0039069

MacNeill, D., Stiehl, G. M., Guimaraes, M. H. D., Buhrman, R. A., Park, J., and Ralph, D. C. (2017a). Control of Spin-Orbit Torques through crystal Symmetry in WTe2/ferromagnet Bilayers. *Nat. Phys.* 13, 300–305. doi:10.1038/nphys3933

MacNeill, D., Stiehl, G. M., Guimarães, M. H. D., Reynolds, N. D., Buhrman, R. A., and Ralph, D. C. (2017b). Thickness Dependence of Spin-Orbit Torques Generated by WTe2. *Phys. Rev. B.* 96, 054450. doi:10.1103/PhysRevB.96.054450

Manchon, A. (2020). Rashba Spin-Orbit Coupling in Two-Dimensional Systems, *Spintronic 2D Materials*, ed. Liu, W.Q. and Xu, Y.B. (Elsevier), 25–64. doi:10.1016/B978-0-08-102154-5.00002-3

Manchon, A., and Zhang, S. (2009). Theory of Spin Torque Due to Spin-Orbit Coupling. *Phys. Rev. B.* 79, 094422. doi:10.1103/PhysRevB.79.094422

Meijer, F. E., Morpurgo, A. F., Klapwijk, T. M., and Nitta, J. (2005). Universal Spin-Induced Time Reversal Symmetry Breaking in Two-Dimensional Electron Gases with Rashba Spin-Orbit Interaction. *Phys. Rev. Lett.* 94, 186805. doi:10.1103/PhysRevLett.94.186805

Mellnik, A. R., Lee, J. S., Richardella, A., Grab, J. L., Mintun, P. J., Fischer, M. H., et al. (2014). Spin-transfer Torque Generated by a Topological Insulator. *Nature* 511, 449–451. doi:10.1038/nature13534

Mermin, N. D., and Wagner, H. (1966). Absence of Ferromagnetism or Antiferromagnetism in One- or Two-Dimensional Isotropic Heisenberg Models. *Phys. Rev. Lett.* 17, 1133–1136. doi:10.1103/PhysRevLett.17.1133

Miron, I. M., Garello, K., Gaudin, G., Zermatten, P.-J., Costache, M. V., Auffret, S., et al. (2011). Perpendicular Switching of a Single Ferromagnetic Layer Induced by In-Plane Current Injection. *Nature* 476, 189–193. doi:10.1038/nature10309

Mogi, M., Tsukazaki, A., Kaneko, Y., Yoshimi, R., Takahashi, K. S., Kawasaki, M., et al. (2018). Ferromagnetic Insulator Cr2Ge2Te6 Thin Films with Perpendicular Remanence. *APL Mater.* 6, 091104. doi:10.1063/1.5046166

Nguyen, M.-H., Ralph, D. C., and Buhrman, R. A. (2016). Spin Torque Study of the Spin Hall Conductivity and Spin Diffusion Length in Platinum Thin Films with Varying Resistivity. *Phys. Rev. Lett.* 116, 126601. doi:10.1103/PhysRevLett.116.126601

Niimi, Y., Morota, M., Wei, D. H., Deranlot, C., Basletic, M., Hamzic, A., et al. (2011). Extrinsic Spin Hall Effect Induced by Iridium Impurities in Copper. *Phys. Rev. Lett.* 106, 126601. doi:10.1103/PhysRevLett.106.126601

Niimi, Y., and Otani, Y. (2015). Reciprocal Spin Hall Effects in Conductors with strong Spin-Orbit Coupling: a Review. *Rep. Prog. Phys.* 78, 124501. doi:10.1088/0034-4885/78/12/124501

Novakov, S., Jariwala, B., Vu, N. M., Kozhakhmetov, A., Robinson, J. A., and Heron, J. T. (2021). Interface Transparency and Rashba Spin Torque Enhancement in WSe2 Heterostructures. *ACS Appl. Mater. Inter.* 13, 13744–13750. doi:10.1021/acsami.0c19266

Ostwal, V., Shen, T., and Appenzeller, J. (2020). Efficient Spin-Orbit Torque Switching of the Semiconducting Van Der Waals Ferromagnet Cr 2 Ge 2 Te 6. *Adv. Mater.* 32, 1906021. doi:10.1002/adma.201906021

Pai, C.-F., Ou, Y., Vilela-Leão, L. H., Ralph, D. C., and Buhrman, R. A. (2015). Dependence of the Efficiency of Spin Hall Torque on the Transparency of Pt/ferromagnetic Layer Interfaces. *Phys. Rev. B.* 92, 064426. doi:10.1103/PhysRevB.92.064426

Park, S. Y., Kim, D. S., Liu, Y., Hwang, J., Kim, Y., Kim, W., et al. (2020). Controlling the Magnetic Anisotropy of the van der Waals Ferromagnet Fe3GeTe2 through Hole Doping. *Nano Lett.* 20, 95–100. doi:10.1021/acs.nanolett.9b03316

Qiu, X., Shi, Z., Fan, W., Zhou, S., and Yang, H. (2018). Characterization and Manipulation of Spin Orbit Torque in Magnetic Heterostructures. *Adv. Mater.* 30, 1705699. doi:10.1002/adma.201705699

Sánchez, J. C. R., Vila, L., Desfonds, G., Gambarelli, S., Attané, J. P., De Teresa, J. M., et al. (2013). Spin-to-charge Conversion Using Rashba Coupling at the Interface between Non-magnetic Materials. *Nat. Commun.* 4, 2944. doi:10.1038/ncomms3944

Schippers, C. F., Swagten, H. J. M., and Guimarães, M. H. D. (2020). Large Interfacial Spin-Orbit Torques in Layered Antiferromagnetic Insulator NiPS3/ferromagnet Bilayers. *Phys. Rev. Mater.* 4, 084007. doi:10.1103/PhysRevMaterials.4.084007

Shao, Q., Yu, G., Lan, Y.-W., Shi, Y., Li, M.-Y., Zheng, C., et al. (2016). Strong Rashba-Edelstein Effect-Induced Spin-Orbit Torques in Monolayer Transition Metal Dichalcogenide/Ferromagnet Bilayers. *Nano Lett.* 16, 7514–7520. doi:10.1021/acs.nanolett.6b03300

Shi, S., Liang, S., Zhu, Z., Cai, K., Pollard, S. D., Wang, Y., et al. (2019). All-electric Magnetization Switching and Dzyaloshinskii-Moriya Interaction in WTe2/ferromagnet Heterostructures. *Nat. Nanotechnol.* 14, 945–949. doi:10.1038/s41565-019-0525-8

Shin, I., Cho, W. J., An, E.-S., Park, S., Jeong, H.-W., Jang, S., et al. (2021). *Spin-orbit Torque Switching in an All-Van der Waals Heterostructure*, 1–19. arXiv [Preprint] Available at: http://arxiv.org/abs/2102.09300.

Song, P., Hsu, C.-H., Vignale, G., Zhao, M., Liu, J., Deng, Y., et al. (2020). Coexistence of Large Conventional and Planar Spin Hall Effect with Long Spin Diffusion Length in a Low-Symmetry Semimetal at Room Temperature. *Nat. Mater.* 19, 292–298. doi:10.1038/s41563-019-0600-4

Soumyanarayanan, A., Reyren, N., Fert, A., and Panagopoulos, C. (2016). Emergent Phenomena Induced by Spin-Orbit Coupling at Surfaces and Interfaces. *Nature* 539, 509–517. doi:10.1038/nature19820

Stiehl, G. M., Li, R., Gupta, V., Baggari, I. E., Jiang, S., Xie, H., et al. (2019a). Layer-dependent Spin-Orbit Torques Generated by the Centrosymmetric Transition Metal Dichalcogenide β–MoTe2. *Phys. Rev. B.* 100, 184402. doi:10.1103/PhysRevB.100.184402

Stiehl, G. M., MacNeill, D., Sivadas, N., El Baggari, I., Guimarães, M. H. D., Reynolds, N. D., et al. (2019b). Current-induced Torques with Dresselhaus Symmetry Due to Resistance Anisotropy in 2D Materials. *ACS Nano.* 13, 2599–2605. doi:10.1021/acsnano.8b09663

Su, T., Lohmann, M., Li, J., Xu, Y., Niu, B., Alghamdi, M., et al. (2020). Current-induced CrI3 Surface Spin-Flop Transition Probed by Proximity Magnetoresistance in Pt. *2d Mater.* 7, 045006. doi:10.1088/2053-1583/ab9dd5

Velický, M., Donnelly, G. E., Hendren, W. R., McFarland, S., Scullion, D., DeBenedetti, W. J. I., et al. (2018). Mechanism of Gold-Assisted Exfoliation of Centimeter-Sized Transition-Metal Dichalcogenide Monolayers. *ACS Nano*. 12, 10463–10472. doi:10.1021/acsnano.8b06101

Walsh, L. A., and Hinkle, C. L. (2017). van der Waals epitaxy: 2D materials and topological insulators. *Appl. Mater. Today.* 9, 504–515. doi:10.1016/j.apmt.2017.09.010

Wang, H., Liu, Y., Wu, P., Hou, W., Jiang, Y., Li, X., et al. (2020a). Above Room-Temperature Ferromagnetism in Wafer-Scale Two-Dimensional van der Waals Fe3GeTe2 Tailored by a Topological Insulator. *ACS Nano.* 14, 10045–10053. doi:10.1021/acsnano.0c03152

Wang, M., Kang, L., Su, J., Zhang, L., Dai, H., Cheng, H., et al. (2020b). Two-dimensional Ferromagnetism in CrTe Flakes Down to Atomically Thin Layers. *Nanoscale* 12, 16427–16432. doi:10.1039/D0NR04108D

Wang, X., Tang, J., Xia, X., He, C., Zhang, J., Liu, Y., et al. (2019). Current-driven magnetization switching in a van der Waals ferromagnet Fe3GeTe2. *Sci. Adv.* 5, eaaw8904. doi:10.1126/sciadv.aaw8904

Wang, Y., Li, L., Yao, W., Song, S., Sun, J. T., Pan, J., et al. (2015). Monolayer PtSe2, a New Semiconducting Transition-Metal-Dichalcogenide, Epitaxially Grown by Direct Selenization of Pt. *Nano Lett.* 15, 4013–4018. doi:10.1021/acs.nanolett.5b00964

Wang, Y., Wang, C., Liang, S. J., Ma, Z., Xu, K., Liu, X., et al. (2020c). Strain-Sensitive Magnetization Reversal of a van der Waals Magnet. *Adv. Mater.* 32, 2004533. doi:10.1002/adma.202004533

Xie, Q., Lin, W., Yang, B., Shu, X., Chen, S., Liu, L., et al. (2019). Giant Enhancements of Perpendicular Magnetic Anisotropy and Spin-Orbit Torque by a MoS 2 Layer. *Adv. Mater.* 31, 1900776–1900779. doi:10.1002/adma.201900776

Xu, H., Wei, J., Zhou, H., Feng, J., Xu, T., Du, H., et al. (2020). High Spin Hall Conductivity in Large-Area Type-II Dirac Semimetal PtTe 2. *Adv. Mater.* 32, 2000513–2000519. doi:10.1002/adma.202000513

Yang, W. L., Wei, J. W., Wan, C. H., Xing, Y. W., Yan, Z. R., Wang, X., et al. (2020). Determining Spin-Torque Efficiency in Ferromagnetic Metals via Spin-Torque Ferromagnetic Resonance. *Phys. Rev. B.* 101, 064412. doi:10.1103/PhysRevB.101.064412

Yim, C., Lee, K., McEvoy, N., O'Brien, M., Riazimehr, S., Berner, N. C., et al. (2016). High-Performance Hybrid Electronic Devices from Layered PtSe2 Films Grown at Low Temperature. *ACS Nano.* 10, 9550–9558. doi:10.1021/acsnano.6b04898

Yu, G., Upadhyaya, P., Fan, Y., Alzate, J. G., Jiang, W., Wong, K. L., et al. (2014). Switching of Perpendicular Magnetization by Spin-Orbit Torques in the Absence of External Magnetic fields. *Nat. Nanotech.* 9, 548–554. doi:10.1038/nnano.2014.94

Zahedinejad, M., Awad, A. A., Muralidhar, S., Khymyn, R., Fulara, H., Mazraati, H., et al. (2020). Two-dimensional Mutually Synchronized Spin Hall Nano-Oscillator Arrays for Neuromorphic Computing. *Nat. Nanotechnol.* 15, 47–52. doi:10.1038/s41565-019-0593-9

Zhang, C., Fukami, S., Watanabe, K., Ohkawara, A., DuttaGupta, S., Sato, H., et al. (2016a). Critical Role of W Deposition Condition on Spin-Orbit Torque Induced Magnetization Switching in Nanoscale W/CoFeB/MgO. *Appl. Phys. Lett.* 109, 192405. doi:10.1063/1.4967475

Zhang, S. (2000). Spin Hall Effect in the Presence of Spin Diffusion. *Phys. Rev. Lett.* 85, 393–396. doi:10.1103/PhysRevLett.85.393

Zhang, W., Sklenar, J., Hsu, B., Jiang, W., Jungfleisch, M. B., Xiao, J., et al. (2016b). Research Update: Spin Transfer Torques in Permalloy on Monolayer MoS2. *APL Mater.* 4, 032302. doi:10.1063/1.4943076

Zhang, W., Wong, P. K. J., Zhu, R., and Wee, A. T. S. (2019). Van der Waals magnets: Wonder building blocks for two-dimensional spintronics? *InfoMat* 1, 479–495. doi:10.1002/inf2.12048

Zhang, Y., Xu, H., Yi, C., Wang, X., Huang, Y., Tang, J., et al. (2021). Exchange Bias and Spin-Orbit Torque in the Fe3GeTe2-Based Heterostructures Prepared by Vacuum Exfoliation Approach. *Appl. Phys. Lett.* 118, 262406. doi:10.1063/5.0050483

Zhou, J., Shu, X., Liu, Y., Wang, X., Lin, W., Chen, S., et al. (2020). Magnetic Asymmetry Induced Anomalous Spin-Orbit Torque in IrMn. *Phys. Rev. B.* 101, 184403. doi:10.1103/PhysRevB.101.184403

Zhou, Y., Jang, H., Woods, J. M., Xie, Y., Kumaravadivel, P., Pan, G. A., et al. (2017). Direct Synthesis of Large-Scale WTe 2 Thin Films with Low Thermal Conductivity. *Adv. Funct. Mater.* 27, 1605928. doi:10.1002/adfm.201605928

Zhu, L., Ralph, D. C., and Buhrman, R. A. (2021). Lack of Simple Correlation between Switching Current Density and Spin-Orbit-Torque Efficiency of Perpendicularly Magnetized Spin-Current-Generator-Ferromagnet Heterostructures. *Phys. Rev. Appl.* 15, 024059. doi:10.1103/PhysRevApplied.15.024059

Zhuo, W., Lei, B., Wu, S., Yu, F., Zhu, C., Cui, J., et al. (2021). Manipulating Ferromagnetism in Few-Layered Cr 2 Ge 2 Te 6. *Adv. Mater.* 33, 2008586. doi:10.1002/adma.202008586

Zollner, K., Gmitra, M., and Fabian, J. (2020a). Swapping Exchange and Spin-Orbit Coupling in 2D van der Waals Heterostructures. *Phys. Rev. Lett.* 125, 196402. doi:10.1103/PhysRevLett.125.196402

Zollner, K., Petrović, M. D., Dolui, K., Plecháč, P., Nikolić, B. K., and Fabian, J. (2020b). Scattering-induced and Highly Tunable by Gate Damping-like Spin-Orbit Torque in

Graphene Doubly Proximitized by Two-Dimensional Magnet Cr2Ge2Te6 and Monolayer WS2. *Phys. Rev. Res.* 2, 043057. doi:10.1103/PhysRevResearch.2.043057

Conflict of Interest: The authors declare that the research was conducted in the absence of any commercial or financial relationships that could be construed as a potential conflict of interest.

The handling Editor declared a past co-authorship with the authors (ZH, YZ).

Publisher's Note: All claims expressed in this article are solely those of the authors and do not necessarily represent those of their affiliated organizations, or those of the publisher, the editors and the reviewers. Any product that may be evaluated in this article, or claim that may be made by its manufacturer, is not guaranteed or endorsed by the publisher.

Copyright © 2021 Tian, Zhu, Jalali, Jiang, Liang, Huang, Chen, Zeng and Zhai. This is an open-access article distributed under the terms of the Creative Commons Attribution License (CC BY). The use, distribution or reproduction in other forums is permitted, provided the original author(s) and the copyright owner(s) are credited and that the original publication in this journal is cited, in accordance with accepted academic practice. No use, distribution or reproduction is permitted which does not comply with these terms.